separations

MDPI

Article

The Effect of Inorganic Mineral Embedding Features in Coking Middling Coals on Their Liberation and Flotation Separation

Yuzhe Hua, Wenli Liu * and Qiming Zhuo

School of Chemical and Environmental Engineering, China University of Mining and Technology (Beijing), Beijing 100080, China

* Correspondence: liuwenli08@163.com; Tel.: +86-13910724272

Abstract

China's coking coal resources are scarce, and maximizing the recycling of these resources is the primary objective of coal processing and utilization. The embedding features of inorganic minerals within coking middling coal resources are an inherent factor influencing their liberation and separation efficiency. However, current research lacks a systematic investigation into how the embedding features of inorganic minerals in coking middling coal affect their liberation characteristics and flotation separation performance. This study examines three Chinese coking middling coal samples with distinct embedding features. Based on quantitative characterization of inorganic mineral embedding, grinding tests with varying durations and flotation separation tests on post-grinding products were conducted. Liberation and separation efficiencies were evaluated to explore the influence of inorganic mineral embedding on liberation degree and the subsequent impact of the liberation degree on flotation performance. The results indicate that the three coking middling coal samples with different embedding features exhibit significant differences in the dissociation behavior between inorganic minerals and organic matter. The particle size (D) of inorganic mineral phases is the primary factor influencing the liberation degree of inorganic minerals, while the complexity of intergrowth between inorganic minerals and organic matter (CIG) is a secondary factor. The CIG is the primary factor affecting the liberation of organic matter. As the liberation of inorganic minerals and organic matter increases, the separation efficiency improves for the Liuwan middling coal samples, whereas it deteriorates for the Shaqu and Changzhi samples.

Keywords: coking middling coal; embedding features; grinding; scanning electron microscopy; degree of liberation; flotation separation

Check for updates

Academic Editor: Qicheng Feng

Received: 1 February 2026
Revised: 23 February 2026
Accepted: 2 March 2026
Published: 4 March 2026

Copyright: © 2026 by the authors. Licensee MDPI, Basel, Switzerland. This article is an open access article distributed under the terms and conditions of the Creative Commons Attribution (CC BY) license.

1. Introduction

With the large-scale extraction of coking coal resources, China's coking coal reserves are progressively declining. However, substantial quantities of coking middling coal continue to be directly utilized as thermal coal for boiler combustion due to its high ash content, resulting in a significant waste of scarce coking coal resources. Consequently, recovering usable coking coal from coking middling coal has attracted considerable attention within the industry [1].To achieve effective separation of inorganic minerals and organic matter in coking middling coal, thorough dissociation of these components is essential. The effectiveness of this dissociation depends on the embedding characteristics of inorganic minerals within the coking middling coal and the grinding process conditions.

Extensive research has been conducted to evaluate the effectiveness of coal crushing and disintegration during coking middling coal [2–10]. This research is primarily based on float–sink tests, utilizing the content of low-density materials in the ground product to characterize the crushing and liberation effects. However, a direct quantitative characterization of the liberation degree of target minerals in the ground product is lacking. Xie et al. [11] investigated the liberation characteristics of coking middling coal under different comminution conditions by analyzing the density distribution of float–sink products. The results demonstrated that grinding products from a jaw crusher achieved superior liberation performance compared to those from a ball mill. Gui et al. [12] investigated the influence of shear angle variation (15°, 30°, 45°, 60°, and 75°) on the comminution and disintegration behavior of coking middling coal using a universal testing machine. Based on the density distribution of float–sink products, they determined that a shear angle of 75° yielded the most effective comminution and disintegration outcomes for coking middling coal. Yue et al. [8] proposed the Coking Coal Liberation Perfection Index (LPI) to quantitatively assess the liberation efficiency of coking middling coal, based on the content of coking middling coal within the 1.4–1.6 g/cm^3 density fraction.

In existing prior research, studies have predominantly focused on coking middling coal from specific coal preparation plants, exploring the fragmentation and liberation patterns of inorganic minerals in coking middling coal solely through macro-scale experiments. Research combining grinding tests with the embedding characteristics of inorganic mineral phases in coking middling coal remains scarce [13]. Studies have shown that operational parameters, such as grinding duration, mill speed, feed material properties, and media characteristics, can significantly affect grinding efficiency [11,14,15]. G. Cheng et al. [16] reported that for coal from the Kailuan mining area, ball milling yielded a finer particle size distribution (PSD), whereas rod milling produced a more uniform PSD. Employing a Box–Behnken design, S. Gautam et al. [17] analyzed the influence of key process parameters—including grinding time, filling rate, feed size, and mill speed—on the fineness of the ground product. The study concluded that all five parameters played a significant role in generating fine particles.

Ground products generally have fine particle sizes, and flotation is widely employed for the separation of inorganic minerals from organic matter [18,19]. However, the flotation process is frequently hindered by phenomena such as mechanical entrainment of fine slimes and slime coating, which degrade separation performance [20,21]. Xia et al. [22] reported that ultrafine kaolinite particles adversely affect coal flotation by reducing suspension surface tension, suppressing bubble coalescence, and stabilizing the froth structure. These effects collectively lead to a higher ash content in the flotation concentrate, which correlates positively with the kaolinite concentration. Cuo et al. [23] investigated the influence of fine slime content on flotation performance. They observed that the presence of fine slime induces both the hooding effect and mechanical entrainment. Consequently, the flotation yield is reduced while the ash content of the concentrate increases. Therefore, developing efficient separation technologies for high-ash fine sludge has become a research priority, as evidenced by studies demonstrating that an optimized reagent regime can effectively mitigate its detrimental effects on flotation performance [24–28]. Sahoo et al. [29] applied an oil flocculation pretreatment to a coal slurry. The flotation results showed that using sunflower oil and castor oil could reduce the ash content of the clean coal product by 7–10%. Chary et al. [24] examined the influence of key parameters—including oil dosage, stirring speed, and flocculation time—on flotation performance in oil flocculation processes. The results demonstrated that optimal performance was achieved under the following conditions: oil dosage of 20%, stirring speed of 1100 rpm, flocculation time of 3 min, and pulp concentration of 4.5%. Ma et al. [30] investigated the role of high-shear pulp

conditioning in the flotation of high-ash fine slimes. Their findings revealed that high-shear conditioning effectively removed fine slimes coating organic particle surfaces, significantly enhanced surface hydrophobicity, and strengthened collector adsorption on the organic particles. Consequently, combustible material recovery was markedly improved, while the reagent dosage required to achieve comparable separation efficiency was substantially reduced. Mei et al. [31] systematically studied the synergistic effect of high-shear pulp preconditioning and PVP flocculant in high-ash fine coal flotation. The results showed that high-shear preconditioning effectively dispersed both inorganic mineral and organic matter particles, while the PVP flocculant selectively promoted the formation of stable organic flocs through bridging mechanisms. This synergistic "dispersion–selective flocculation" process reduced the concentrate ash content to 12.74% and increased the combustible recovery to 66.26%, offering an effective technical route for the efficient separation of high-ash fine coal.

In summary, while significant research has examined the effects of grinding conditions on comminution and liberation, as well as the influence of flotation parameters on separation efficiency, the impact patterns of inorganic mineral embedding features in coking middling coal on liberation efficiency—and subsequently, the effects of mineral liberation degree on separation performance—remain largely unexplored and poorly understood. To address this gap, the present study builds on previous research on the quantitative characterization of inorganic mineral embedding features. Using three Chinese coking middling coals with distinct mineral embedding features as test materials, scanning electron microscopy (SEM) and image processing techniques were applied to determine the liberation degrees of inorganic minerals and organic matter in each grinding product. Based on these measurements, the influence patterns of inorganic mineral embedding features on liberation efficiency were elucidated. Furthermore, flotation tests conducted on ground products with varying liberation degrees were used to systematically investigate the impact of the liberation degree on the separation efficiency of both inorganic minerals and organic matter.

2. Research Methods

This research primarily focuses on three aspects, as illustrated in Figure 1: quantitative characterization of inorganic mineral embedding features in coking middling coal, grinding tests at different time intervals and calculation of product liberation degree, and flotation separation of ground products with different liberation degrees.

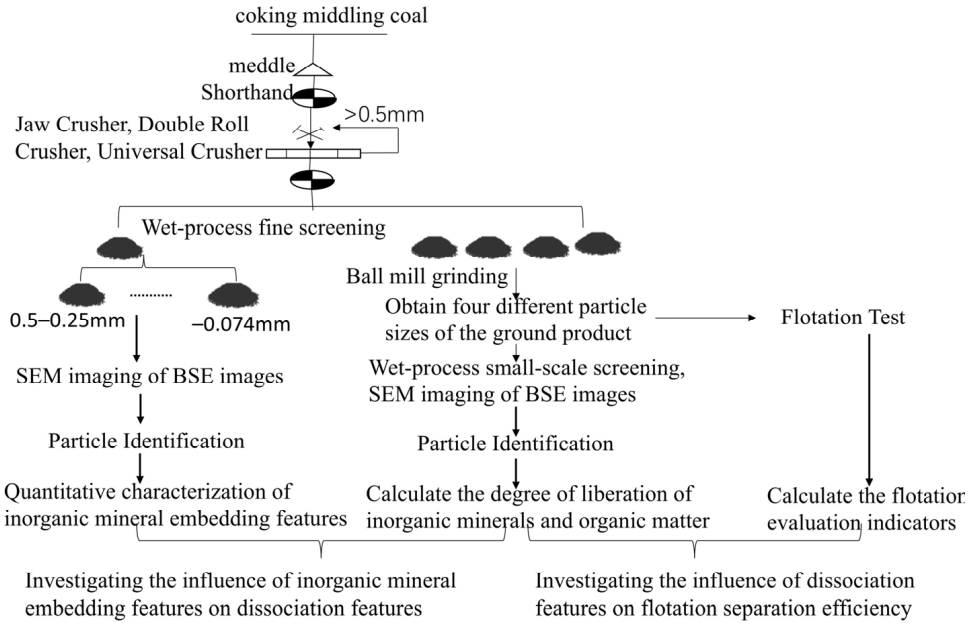


Figure 1. Experimental flowchart.

2.1. Preparation of Test Specimens

Shanxi serves as a significant production base for coking coal in China. Eleven coking middling coal samples were collected from various regions across Shanxi. In previous work [13], the authors qualitatively analyzed the mineral embedding characteristics of these samples, focusing on three dimensions: the embedding features of inorganic minerals—including their particle size, morphology, and degree of intergrowth with organic matter. Based on this analysis, three representative coking middling coal samples were selected for the present study: Liuwan coking middling coal (LW), Changzhi coking middling coal (CZ), and Shaqu coking middling coal (SQ). Industrial and elemental analyses were performed on these three representative coking middling coals, and the results are summarized in Table 1. Industrial analysis was conducted on three representative coking middling coals according to Industrial Analysis Methods for Coal. Elemental analysis was performed on each sample using an elemental analyzer, with the results shown in Table 1.

Table 1. Results of industrial analysis and elemental analysis of coking middling coal.

Name	Industrial Analysis (%)				Elemental Analysis (%)				
	Ash	Moisture	Volatile Matter	Fixed Carbon	C	H	O	N	S
LW	31.13	1.15	32.61	35.11	86.50	2.66	8.66	0.94	1.24
CZ	36.85	0.46	16.07	47.61	79.43	2.74	16.62	1.02	0.20
SQ	39.46	0.55	16.22	43.77	81.41	2.89	14.43	0.74	0.53

2.2. Grinding Test

Grinding tests were performed on the three coking middling coals using a WZM-Horizontal Ball Mill (WZM Dingshu Haoqiang Machinery Factory, Wuxi, China) operated for different durations. The specific grinding parameters are provided in Table 2.

Table 2. Parameters for grinding tests.

Parameters	Parameter Settings
Feed (g)	93.29
Medium Material	Zirconium Oxide
Medium Shape	Spherical
Medium Ratio	15 mm:10 mm:6 mm = 1:1:1
Medium Weight (kg)	1.5
Speed Ratio (%)	75

Each ground product was subjected to wet sieving using screens with apertures of 0.25, 0.125, 0.074, and 0.045 mm, resulting in five narrowly sized fractions. The weighted average particle size (d) of each ground product was then calculated according to Formula (1).

$$d = \frac{\sum_{i=1}^{5} \frac{d_{imax}+d_{imin}}{2} \times w_i}{\sum_{i=1}^{5} w_i} \quad (1)$$

i: the i-th sieve for the narrow particle size fraction; w_i: yield of the i-th sieve for the narrow particle size fraction; d_{imax}: upper limit particle size of the i-th sieve for the narrow particle size fraction; and d_{imin}: lower limit particle size of the i-th sieve for the narrow particle size fraction.

Based on the weighted average particle size (d) of each ground product, a relational model between the particle size of the ground coking middling coal and grinding duration was established. This model was subsequently applied to determine the grinding times

required to achieve target average particle sizes of 100, 60, 40, and 30 μm for the three ground coking middling coals, as summarized in Table 3.

Table 3. Grinding time required for three coking middling coals to achieve a specific particle size.

Particle Size *d* (μm) of Ground Product	Grinding Time Required to Achieve a Specific Particle Size (min)		
	LW	CZ	SQ
100	5	5	6
60	15	15	17
40	40	30	60
30	120	90	120

Following the grinding durations specified in Table 3, grinding tests were carried out on the three coking middling coals, producing ground products with target average particle sizes of 100, 60, 40, and 30 μm. Wet sieving was performed on the resulting 12 ground products, generating 60 narrowly sized fractions for subsequent SEM imaging analysis.

2.3. Acquisition and Processing of BSE Images of Ground Products

Thin sections suitable for SEM observation were prepared from each narrow-size fraction sample. Backscattered electron (BSE) imaging (ZEISS Sigma 360, Carl Zeiss, Oberkochen, Germany) was then performed on these sections, yielding over 1500 BSE images in total. Using image processing software, individual inorganic mineral grains, discrete organic matter particles, intergrown particles, and embedded inorganic mineral phases were identified and quantified across the 60 narrow-size fraction samples. Representative occurrences of these particle types are illustrated in Figure 2.

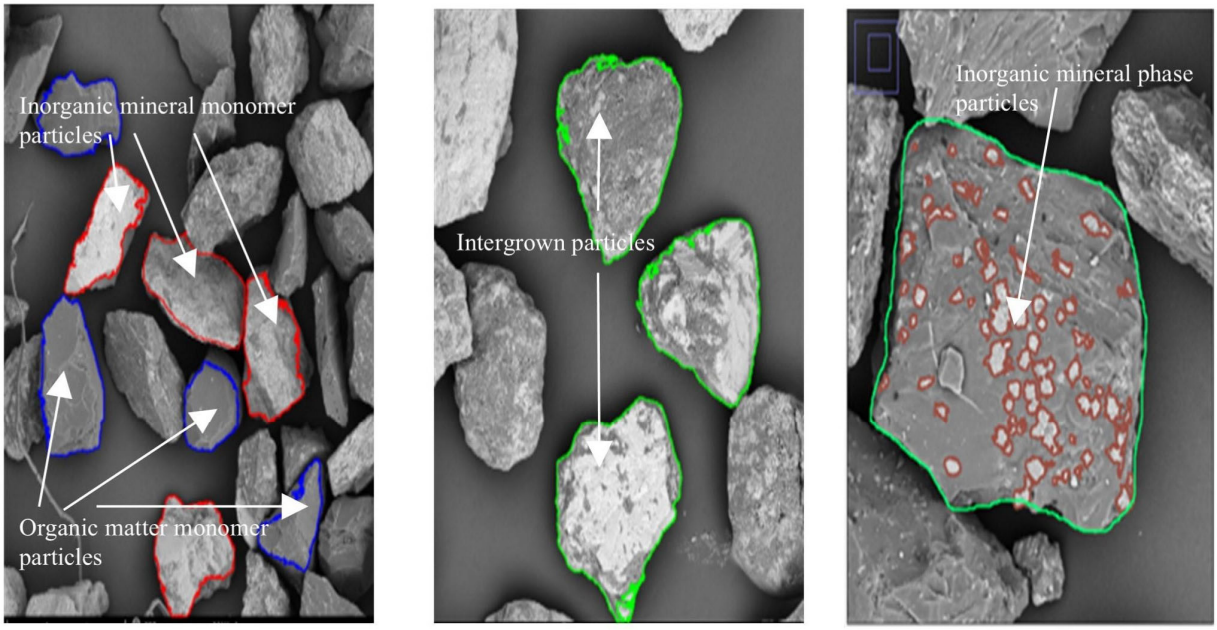


Figure 2. Different types of particles in coking middling coal.

The accuracy of quantitatively characterizing the dissociation of inorganic minerals and organic matter critically depends on the number of particles identified within each narrow-size fraction. An insufficient particle count compromises statistical representativeness. To establish a reliable benchmark, the authors previously investigated the convergence

behavior of the mean particle area as a function of increasing particle count [13]. By progressively expanding the sample size until the mean value stabilized within a 95% confidence interval, a minimum particle count satisfying the statistical requirements was determined, thereby providing a foundation for precise liberation analysis. Following this approach, the present study identified over 128,000 particles across all categories in BSE images from 60 narrow-size fraction samples. Specifically, the LW, CZ, and SQ samples yielded approximately 43,000, 44,000, and 41,000 particles, respectively, ensuring the robustness and comparability of subsequent statistical analyses.

2.4. Calculation of the Degree of Liberation of Inorganic Minerals and Organic Matter in Ground Products

Organic matter constitutes 60–70% of coking coal, and clay minerals account for approximately 90% of the inorganic fraction [32,33]. Therefore, it is sufficient to treat the various types of inorganic minerals as a single, unified group for this study. In previous research [13], quantitative characterization methods for the mineral embedding features of coking middling coal were developed, leading to the proposal of three suitable descriptive parameters: the equivalent diameter (D) and the aspect ratio (AR) of inorganic mineral phases, along with the complexity of inorganic–organic intergrowth (CIG). In this study, D represents the two-dimensional equivalent diameter of inorganic mineral phases, providing a quantitative measure of their size distribution. AR, defined as the ratio of the longest to the shortest axis, characterizes the elongation and morphological irregularity of these mineral particles. CIG, a parameter calculated via the entropy method, integrates the area, number, and associated intergrown particle area of the inorganic mineral phases to quantify the complexity of their intergrowth with organic matter. Utilizing the methodology described above, the embedding features of inorganic minerals within three coking middling coals were quantitatively characterized. The corresponding results are summarized in Table 4.

Table 4. Inorganic mineral embedding features of three coking middling coals.

Name	D (μm)	AR	CIG (%)
LW	15.23	1.97	32.32
CZ	5.11	1.91	62.52
SQ	5.40	1.90	70.14

In this study, the degree of liberation for both inorganic minerals and organic matter is herein defined as the proportion of a component's total surface area that exists as liberated monomers. First, using Formulas (2) and (3), the degrees of liberation of inorganic minerals (LM_{ij}) and organic matter (LO_{ij}) were calculated for each narrow-size fraction of the three coking middling coals. The areas of liberated inorganic minerals, liberated organic matter, intergrown inorganic minerals, and intergrown organic matter in each narrow-size fraction were obtained using the method described in Section 2.3. Subsequently, the overall degrees of liberation of inorganic minerals (TLM_i) and organic matter (TLO_i) in each ground product of the three coking middling coals were calculated using Formulas (4) and (5).

The liberation degree of inorganic minerals in coking middling coals is governed by their embedding features during the grinding process. To quantify the impact of these embedding features on the liberation of both inorganic minerals and organic matter, two evaluation metrics are introduced: percentage increase in inorganic mineral liberation

content (CLM_p) and percentage increase in organic matter liberation content (CLO_p). The calculation methods are shown in Equations (6) and (7), respectively.

$$LM_{ij} = \frac{S_{MM_{ij}}}{S_{MM_{ij}} + S_{IM_{ij}}} \times 100 \quad (2)$$

$$LO_{ij} = \frac{S_{MO_{ij}}}{S_{MO_{ij}} + S_{IO_{ij}}} \times 100 \quad (3)$$

$$TLM_i = \frac{\sum_{j=1}^{5} LM_i \times W_j}{100} \quad (4)$$

$$TLO_i = \frac{\sum_{j=1}^{5} LO_i \times W_j}{100} \quad (5)$$

$$CLM_p = \frac{\Delta TLM_i}{\Delta TLM_{100-30}} \times 100 \quad (6)$$

$$CLO_p = \frac{\Delta TLO_i}{\Delta TLO_{100-30}} \times 100 \quad (7)$$

LM_{ij}, LO_{ij}: in the j-th sieve fraction of the i-th ground product, degree of liberation of inorganic minerals, degree of liberation of organic matter (%); $S_{MM_{ij}}, S_{MO_{ij}}$: in the j-th sieve fraction of the i-th ground product, area of inorganic mineral monomers and area of organic matter monomers (μm^2); and $S_{IM_{ij}}, S_{IO_{ij}}$: in the j-th sieved narrow-grain fraction sample of the i-th ground product, the area of intergrowth inorganic minerals and the area of intergrowth organic matter (μm^2). TLM_i, TLO_i: The i-th ground product, inorganic mineral liberation degree and organic matter liberation degree (%). CLM_p, CLO_p: the p-th grinding stage—percentage increase in inorganic mineral liberation content and percentage increase in organic matter liberation content (%); $\Delta TLM_j, \Delta TLO_j$: incremental values of inorganic mineral liberation and organic matter liberation (%) between the $(i + 1)$th and i-th post-grinding products.

2.5. Floating Test of Three Coking Medium Coal Grinding Samples and Their Post-Grinding Products

Unit flotation tests were conducted using an XFD-1 laboratory flotation machine (Mingrong Mining Machinery Equipment Co., Ltd., Ganzhou, China) on both the feed samples and the ground products (with average particle sizes of 100, 60, 40, and 30 μm) of three coking middling coals (LW, CZ, and SQ). The tests were performed at varying collector dosages while maintaining consistent equipment parameters and process conditions throughout the experiment, as illustrated in Figure 3. The frother, 2-Octanol, was added at a fixed dosage of 80 g/t, whereas the collector, dodecane, was varied at 1000, 600, 200, 100, and 50 g/t.

This research seeks to produce clean coking coal meeting target ash specifications by leveraging flotation techniques. Traditional indicators for combustible recovery rate and flotation optimization—which emphasize recovery efficiency and proximity to theoretical limits—are unsuitable for evaluating the separation effectiveness of this flotation process. Therefore, this paper employs coking coal yield and ash content as metrics for assessing flotation separation performance.

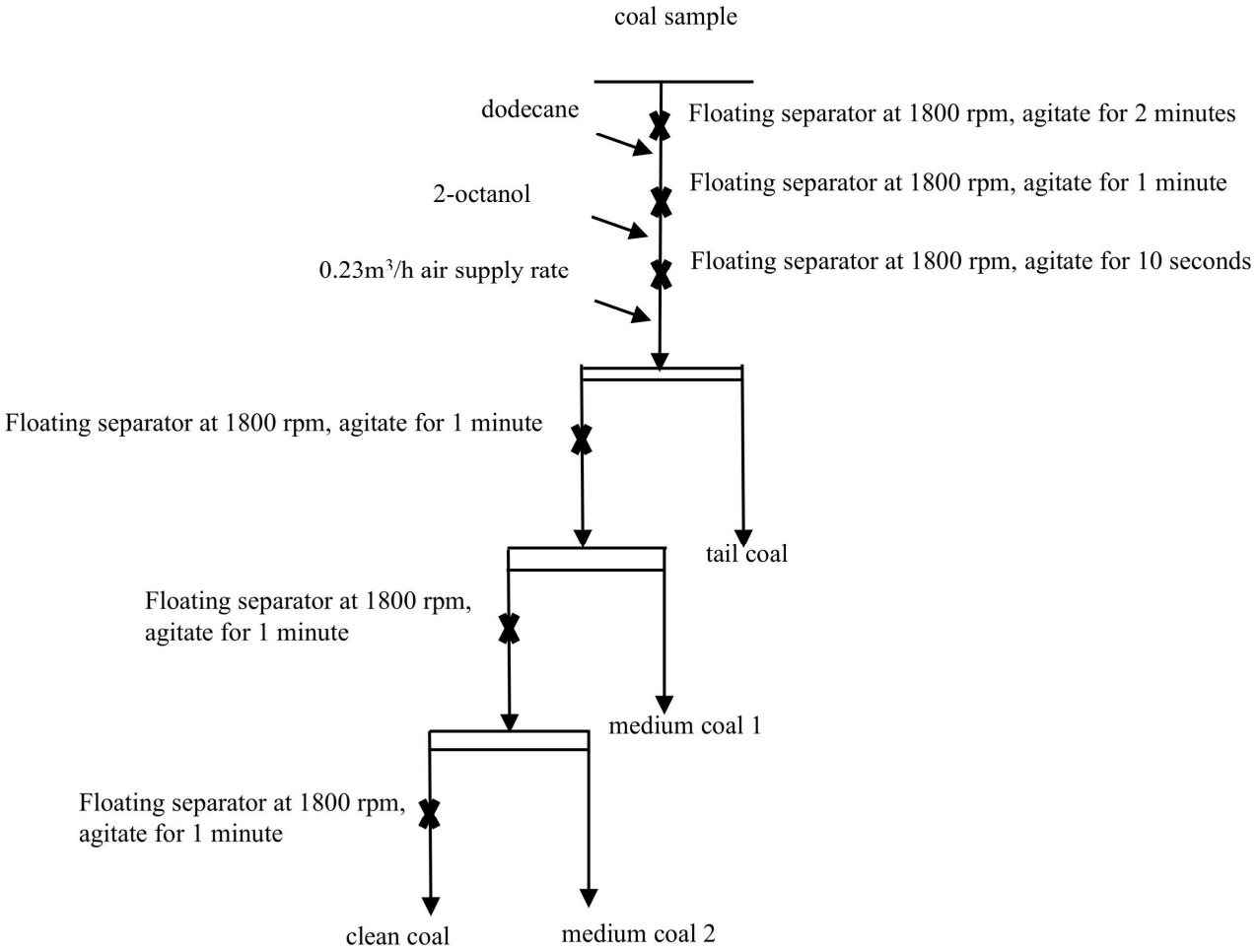


Figure 3. Flotation process flowchart.

3. Results Analysis

3.1. Features of Inorganic Mineral Liberation in Three Coking Middling Coals

To visually demonstrate the significant differences in the inorganic mineral liberation features among the three coking middling coals, representative BSE images were selected for comparative analysis, as shown in Figure 4. Following the methodology outlined in Section 2.4, the liberation degrees of inorganic minerals in the ground products of the three coking middling coals were quantified. The analysis of liberation degree variations relative to grinding fineness is illustrated in Figure 5a,b. Furthermore, to elucidate the underlying mechanisms governing the disparities in liberation, a quantitative correlation between embedding feature parameters and liberation degree changes was constructed, as depicted in Figure 5c–e.

As shown in Figure 4, the three coking middling coals exhibit markedly different degrees of separation between inorganic minerals and organic matter after grinding. Notably, the number of intergrown particles containing embedded inorganic mineral phases is substantially lower in CZ compared to LW and SQ, suggesting that CZ achieves the highest level of inorganic mineral liberation. In contrast, LW is characterized by the presence of coarse-grained inorganic mineral phases, whereas SQ contains fine-grained and numerous inorganic mineral particles. In such cases, a precise determination of the inorganic mineral liberation degree necessitates quantitative characterization.

As illustrated in Figure 5a,b, the degree of inorganic mineral liberation in the three coking middling coals shows distinct variation trends as the particle size of the ground product decreases.

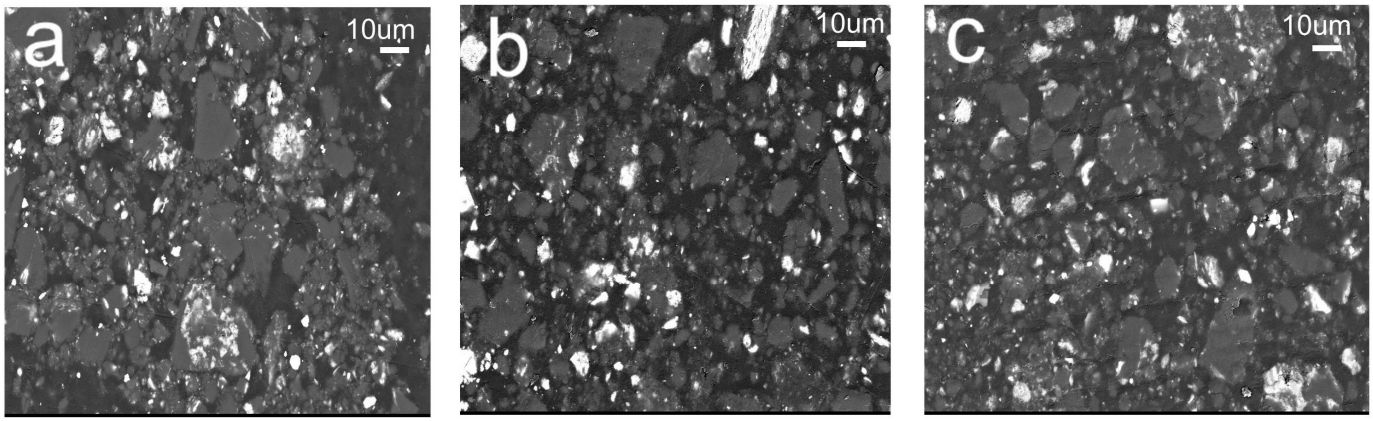


Figure 4. Representative BSE images of the −0.045 mm size fractions of the three coking middling coals ground to an average particle size of 30 μm: (**a**) LW; (**b**) CZ; (**c**) SQ.

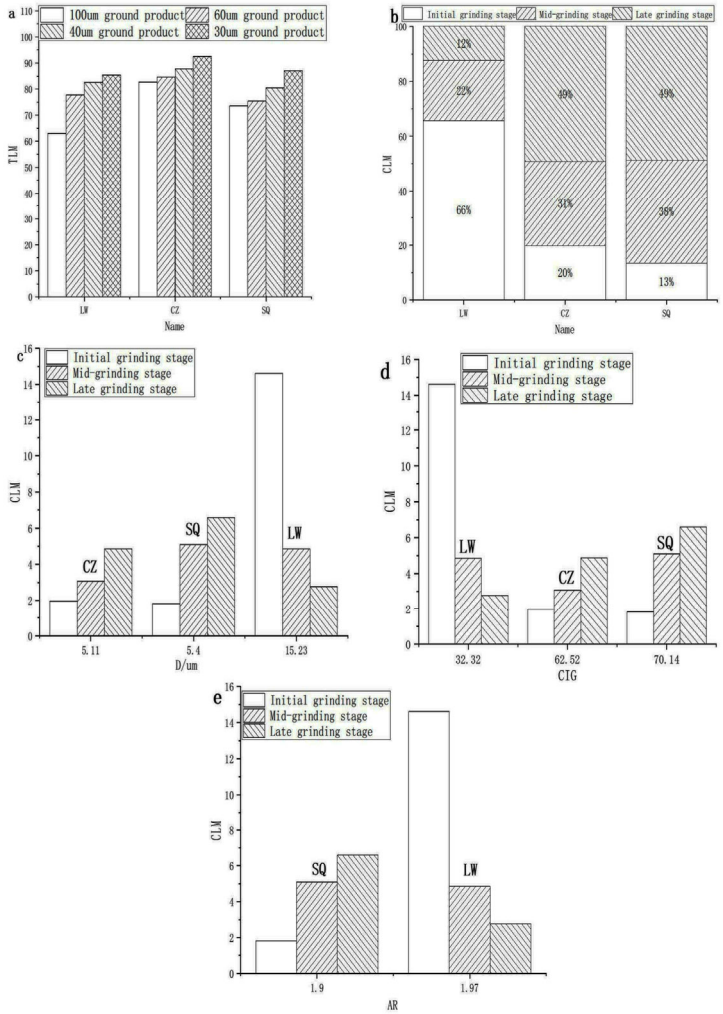


Figure 5. Dissociation features of inorganic minerals in the ground products of three coking middling coals. (**a**) Degree of liberation of inorganic minerals (TLM) in the ground products of three coking middling coals. (**b**) Percentage increase in inorganic mineral liberation content (CLM) at each grinding stage for three coking middling coals. (**c**–**e**) The effect of three coking middling coals' embedding features parameters (D, CIG, AR) on the CLM.

(1) When the ground products of the three coking middling coals reached a particle size of 100 μm, the inorganic mineral liberation degrees for CZ, SQ, and LW were 82.68%, 73.55%, and 63.10%, respectively. The liberation degree of discrete inorganic mineral

particles in CZ was significantly higher than that in SQ and LW. This indicates that at this particle size, most inorganic minerals in CZ had achieved effective liberation, whereas a substantial portion of inorganic minerals in LW remained unliberated. The difference is visually reflected in the distinct distribution ratios between discrete and intergrown inorganic mineral particles. Inorganic minerals in CZ predominantly exist as discrete particles, while those in LW mainly occur as intergrown particles embedded within the organic matrix.

(2) When the three coking middling coals were ground from 100 μm to 40 μm, the inorganic mineral liberation degree increased by 22.23% for LW, 13.50% for SQ, and 9.91% for CZ. For LW, the majority of the increase in mineral dissociation occurred during the initial grinding stage (ground product average size: 100–60 μm), contributing about 66% of the total liberation gain in this period. In contrast, for CZ and SQ, the main increase took place in the later grinding stage (ground product average size: 40–30 μm), which accounted for approximately 50% of the total liberation increase over the entire grinding process.

(3) When the ground product reached a particle size of 30 μm, the inorganic mineral liberation degrees for CZ, SQ, and LW were 92.59%, 87.05%, and 85.33%, respectively. The differences in inorganic mineral liberation among the three coking middling coals became notably smaller. CZ continued to show higher discrete-particle liberation than SQ and LW. It is noteworthy that the liberation degree of LW at this particle size was only 2.68 percentage points higher than that of CZ at 100 μm.

In summary, among the three coking middling coals, CZ consistently exhibited the highest inorganic mineral liberation degree across all ground products, exceeding 82% (with a maximum of 92.59%). SQ and LW showed generally lower liberation degrees, surpassing 82% only when the ground product reached a particle size of 30 μm. Although LW displayed the lowest inorganic mineral liberation (as low as 63.10%) at a ground product size of 100 μm, its liberation increased markedly (by 22.23 percentage points) as the particle size decreased. This reduced the gap in liberation among the three coking middling coals from 19.58% to 7.26%. Specifically, LW achieves rapid inorganic mineral liberation mainly during the initial grinding stage (100–60 μm), whereas CZ and SQ exhibited concentrated liberation in the later grinding stage (40–30 μm).

As shown in Figure 5c–e, the underlying cause for the notable differences in the dissociation behaviors of inorganic minerals among the three coking middling coals is attributed to their distinct intrinsic mineral embedding features.

(1) For LW inorganic minerals, which have a mean grain size of approximately 15.23 μm, effective liberation can be achieved by grinding the sample to around 60 μm. In contrast, for CZ and SQ inorganic minerals with mean grain sizes near 5 μm, deep grinding to about 30 μm is required to attain efficient liberation. This observation aligns with the theoretical principle that coarser inorganic mineral phases liberate more readily during comminution. This occurs because particle fracture typically initiates at the weakest points within the structure, with boundaries between different phases being preferentially broken under grinding stress [34]. At the same grinding fineness, the coarser mineral grains in LW favor fracture along the mineral–organic intergrowth interfaces, thereby enhancing inorganic mineral liberation. For the finer-grained minerals in CZ and SQ, grinding forces are more likely to penetrate entire intergrown particles, causing simultaneous breakage of both inorganic minerals and organic matter. This generates a greater number of fine intergrown fragments, which lowers the overall degree of inorganic mineral liberation.

(2) When the complexity of inorganicorganic intergrowth (CIG) exceeds 60%, samples require deep grinding to achieve effective liberation. The CIG value for LW inorganic minerals is 32.32%, reflecting a relatively simple intergrowth structure with organic matter. As a result, LW inorganic minerals readily achieve discrete liberation during the initial

grinding stage (100–60 μm). In contrast, CZ and SQ inorganic minerals both exhibit CIG values greater than 60%, indicating a highly complex association with the organic matrix. Consequently, significant liberation of inorganic minerals in these two coking middling coals occurs only in the later grinding stage (40–30 μm). This is because in coking middling coals with complex mineral–organic intergrowth, inorganic mineral particles are either finely disseminated or present in high particle counts, necessitating more intensive grinding to break the intricate interfacial bonding and promote liberation.

(3) The embedding morphology (aspect ratio, AR) of inorganic mineral phase particles exerts a relatively limited influence on their liberation degree. Among the three coking middling coals, the AR values of inorganic mineral phases in CZ and SQ are similar; thus, these two samples are grouped together for comparison with LW. The AR of LW's inorganic mineral phases was 1.97, higher than the 1.90 recorded for CZ and SQ. Correspondingly, LW exhibited a notably larger increase in inorganic mineral liberation than CZ and SQ. This difference arises because, under comparable particle size conditions, vein-like (higher-AR) mineral phases tend to liberate more readily. When grinding forces act on equant (lower-AR) mineral aggregates, stress distributes relatively uniformly over the particle surface. In contrast, when applied to elongated or vein-like (higher-AR) particles, stress concentrates preferentially at edges or tips. This localized stress concentration promotes fracture along the mineral–organic interface, thereby enhancing the detachment of inorganic minerals from the organic matrix.

In summary, the particle size (D) of inorganic mineral phases is the dominant factor governing the degree of inorganic mineral liberation, while the complexity of inorganic–organic intergrowth (CIG) serves as a secondary influencing factor.

3.2. Features of Organic Matter Liberation in Three Coking Middling Coals

The liberation process of coking middling coals involves the separation of inorganic minerals from organic matter. The liberation behavior of both phases jointly determines subsequent flotation performance, making the study of organic matter liberation equally important. Following the calculation method described in Section 2.4, the organic matter liberation degree was systematically determined for each ground product of the three coking middling coals, and its variation with grinding particle size was analyzed (Figure 6a,b). To elucidate the mechanisms underlying the differences in organic matter liberation among the three coking middling coals, quantitative relationships were established between the inorganic mineral embedding parameters and the corresponding liberation degree variations (Figure 6c–e). Among these parameters, the complexity of inorganic–organic intergrowth (CIG) directly describes the intergrowth state between organic and inorganic phases; its influence mechanism will therefore be the focus of analysis.

As shown in Figure 6a,b, the variation in organic matter liberation degree among the three coking middling coals displays distinct trends as the particle size of the ground product decreases.

(1) Among the three coking middling coals, the ground products of CZ showed the highest organic matter liberation degree, followed by LW, with SQ exhibiting the lowest. At a particle size of 30 μm, the organic matter liberation degrees for CZ, LW, and SQ were 64.13%, 58.97%, and 38.89%, respectively.

(2) When the particle size of the ground product decreased from 100 μm to 30 μm, the liberation degree of organic matter monomers in LW, CZ, and SQ increased by 39.47%, 31.68%, and 24.23%, respectively. For LW and CZ, most of the increase in organic matter liberation occurred during the initial grinding stage, with the subsequent stage contributing a relatively smaller portion. The liberation growth in these two periods accounted for 82% and 96% of the total increase, respectively. In contrast, for SQ, the predominant increase in

organic matter liberation took place during the later grinding stage, during which the rise in liberation accounted for 47% of the total increase observed in that stage.

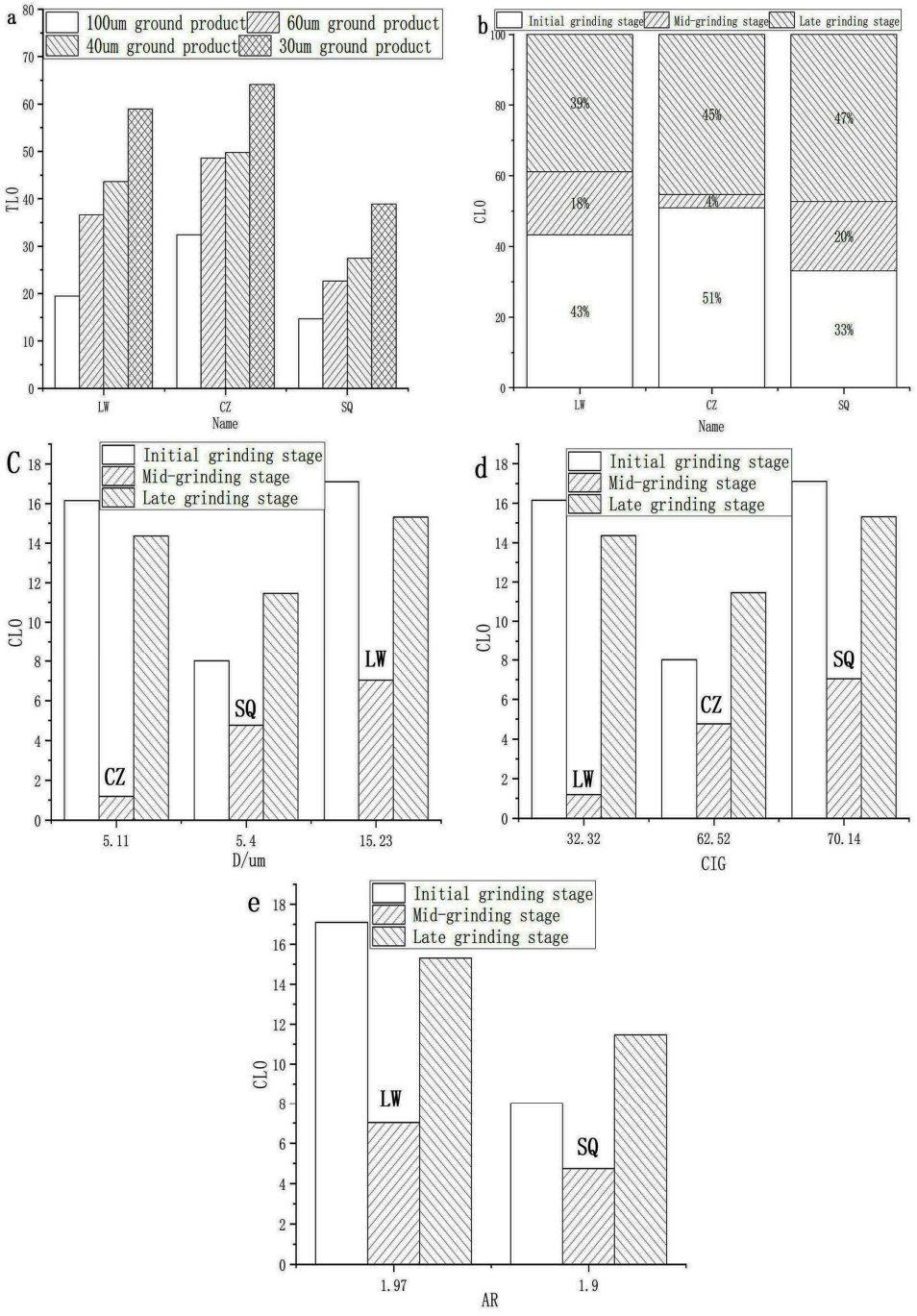


Figure 6. Dissociation features of organic matter in the ground products of three coking middling coals. (**a**) Degree of liberation of organic matter (TLO) in the ground products of three coking middling coals. (**b**) Percentage increase in organic matter liberation content (CLO) at each grinding stage for three coking middling coals. (**c–e**) The effect of three coking middling coals' embedding feature parameters (D, CIG, AR) on the CLO.

As shown in Figure 6c–e, the distinct inorganic mineral embedding features of the three coking middling coals influenced their organic matter liberation behavior.

(1) The particle size (D) and grain morphology (aspect ratio, AR) of inorganic mineral phases exert only a limited influence on the degree of organic matter liberation.

(2) When the complexity of inorganic–organic intergrowth (CIG) is 32.32% in LW, the organic matter liberation degree increases by 39.47%. In contrast, when the CIG reaches 70.14% in SQ, the liberation degree increases by only 24.23%. This difference arises because organic matter liberates more readily when the associated inorganic minerals are coarser in grain size or lower in abundance.

In summary: (1) Among the three coking middling coals, CZ consistently exhibited the highest organic matter liberation degree across all ground products. As particle size decreased, efficient liberation of organic matter in LW and CZ occurred predominantly during the initial grinding stage, with further liberation in the later stage; in SQ, efficient liberation was concentrated mainly in the later grinding stage. (2) The complexity of inorganic–organic intergrowth (CIG) is the dominant factor governing the degree of organic matter liberation.

3.3. Flotation Test Results for Three Coking Middling Coals Grinding Samples and Their Post-Grinding Products

Using the flotation method detailed in Section 2.5 (constant frother dosage and process flow), this study examined how collector dosage affects the flotation of ground products with different liberation levels. The degree of liberation is theorized to be a key factor influencing both reagent consumption and separation efficiency. Specifically, a lower collector dosage improves selectivity for poorly liberated products, reducing concentrate ash. In contrast, well-liberated materials, with their extensive fresh hydrophobic surfaces, require a higher collector dosage to maintain ash levels while boosting yield. Following the flotation test methodology outlined in Section 2.5, this study performed flotation experiments at varied reagent dosages on both mill feed samples and ground products of different particle sizes (100, 60, 40, and 30 μm) from the three coking middling coals. The corresponding results are provided in Tables A1–A3 in the Appendix A. To further clarify the impact of inorganic mineral liberation on flotation performance, quantitative relationships between the inorganic mineral liberation degree and key flotation indicators (clean coal ash and clean coal yield) were established, as shown in Figure 7.

As shown in Figure 7, (1) among the three coking middling coals, a slight decrease in concentrate ash content with reduced collector dosage was observed when the average product particle size exceeded 40 μm. However, this trend did not hold for particle sizes below 40 μm, where collector dosage showed no significant effect on concentrate ash—a finding that deviates from theoretical expectations. This discrepancy can be attributed to the fact that, as the ground product becomes finer, the liberated inorganic mineral particles enter the ultrafine size range. In this regime, the dominant mechanisms governing flotation shift from selective reagent adsorption to hydrodynamic forces and interfacial interactions. Under such conditions, fine mineral particles are entrained non-selectively into the concentrate via fine-sliming and mechanical entrainment, effects that cannot be effectively mitigated by simply adjusting collector dosage alone.

(2) At a collector dosage of 100 g/t, the ash content of the LW flotation concentrate first decreased and then increased with rising inorganic mineral liberation, while the concentrate yield followed an opposite trend, first increasing and then decreasing. When inorganic mineral liberation reached 63.10%, the concentrate ash content reached its lowest value of 15%, accompanied by a concentrate yield of 23.59%. Theoretically, finer grinding enhances liberation and should thus improve flotation performance. Nevertheless, the LW flotation results indicate that separation efficiency generally declines as the ground product particle size decreases. Notably, when the ground product size reached 30 μm, the separation indices under different reagent dosages converged at similarly low levels. This discrepancy can likely be attributed to the fact that, although finer grinding increases liberation, the resulting particle size (below 60 μm) falls outside the effective flotation range for coal slurry

(typically 0.5–0.074 mm). Excessively fine particles are prone to mechanical entrainment and slime coating, which compromise separation selectivity and overall efficiency.

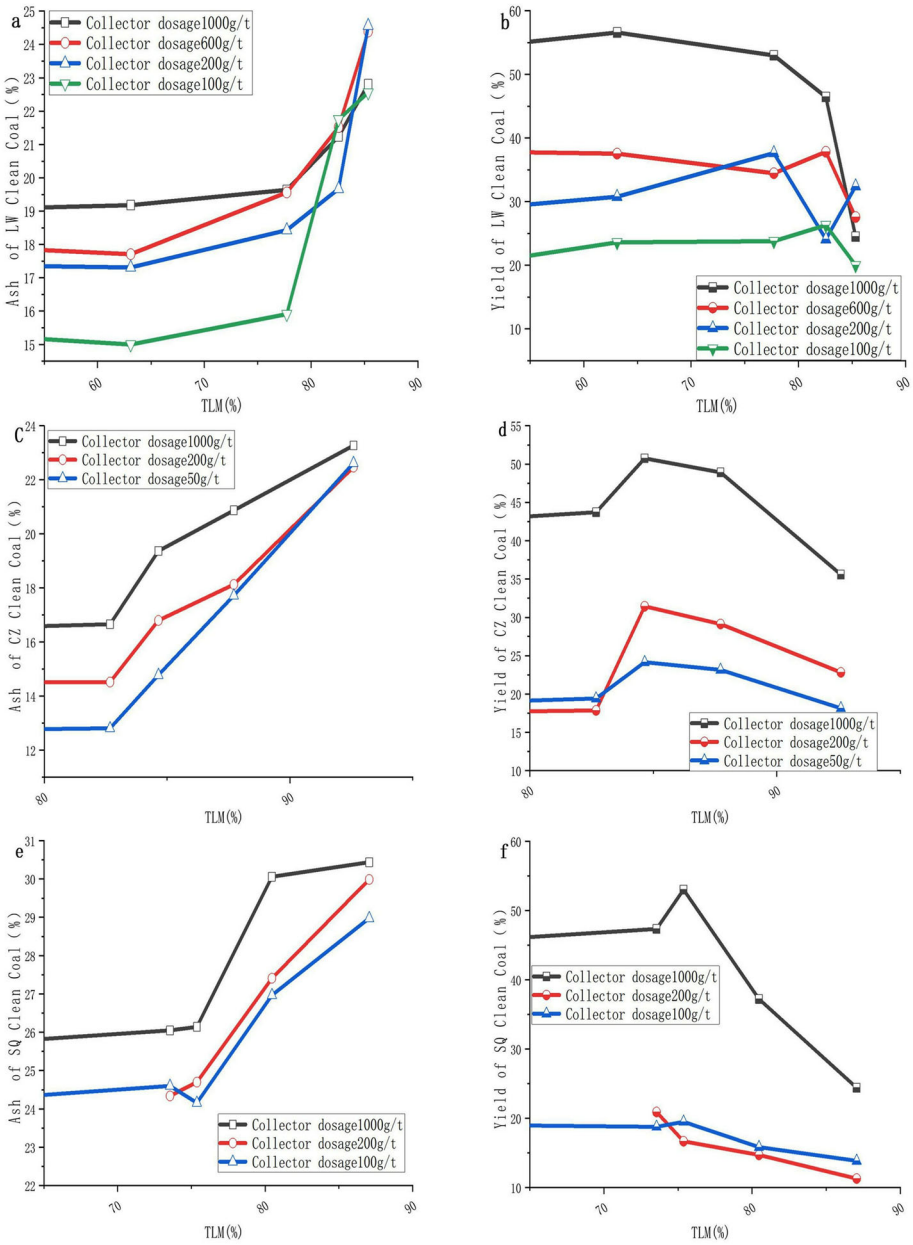


Figure 7. The variation patterns of flotation evaluation metrics in relation to the liberation degree of inorganic minerals for the three coking middling coals and their respective ground products under different collector dosages. (**a**,**c**,**e**) illustrate the ash content of the flotation concentrates and (**b**,**d**,**f**) depict the yield of the flotation concentrates.

(3) At a collector dosage of 50 g/t, the ash content of the flotation concentrate from CZ gradually increased as the ground product's particle size decreased, while the concentrate yield first rose and then declined. The feed sample exhibited the lowest ash content (11.94%) and a concentrate yield of 11.20%. Consistent with the observed decline in flotation performance for LW as grinding proceeded, the separation results for CZ at an average ground product size of 100 μm were poorer than those of the feed sample. This deterioration likely originates from the inherently fine particle size distribution of inorganic mineral phases in CZ. As a result, liberated organic matter particles also remain fine, which promotes slime entrainment and coating, thereby reducing separation efficiency.

(4) At a collector dosage of 100 g/t, the ash content of the flotation concentrate from SQ gradually increased as the ground product particle size decreased, while the concentrate yield showed a declining trend. Among all samples, the ground feed exhibited the lowest concentrate ash content (22.58%) and a corresponding yield of 19.49%. In line with the previously observed deterioration in flotation performance for CZ as grinding progressed, SQ displayed a similar pattern. This consistency suggests that the adverse effect of fine grinding on separation efficiency is not limited to a single type of middling but may be a common response in materials where liberated inorganic and organic particles both fall into sizes prone to entrainment and slime interference.

In summary, among the three coking middling coals, ground CZ exhibited the highest degree of organic matter liberation, followed by LW, with SQ showing the lowest. Correspondingly, the ash content of the cleaned coal products followed a consistent trend: CZ had the lowest ash content, LW was intermediate, and SQ displayed the highest ash content. For coking middling coal with distinct embedding and liberation features, future research urgently requires a holistic perspective to enable multidimensional process optimization tailored to its degree of liberation. This entails not only the development of compound flotation reagent systems—such as the introduction of novel high-selectivity collectors and flocculants—but also the restructuring of flotation process flows, including classified flotation for coarse coal slimes and microbubble flotation for ultrafine fractions. Only by deeply integrating liberation parameters into the separation process can the existing technical bottlenecks be ultimately overcome, achieving efficient and selective separation of inorganic minerals from organic matter in coking middling coal.

4. Conclusions

(1) Among the three coking middling coals, the ground products of CZ consistently showed the highest inorganic mineral liberation degree, all exceeding 82% (with a peak of 92.59%). SQ and LW generally exhibited lower inorganic mineral liberation, surpassing 82% only when the ground product reached a particle size of 30 μm.

(2) The rapid increase in inorganic mineral liberation for LW occurred mainly during the initial grinding stage (100–60 μm), whereas CZ and SQ achieved concentrated liberation during the later grinding stage (40–30 μm). The analysis indicates that the particle size (D) of inorganic mineral phases is the dominant factor governing inorganic mineral liberation, while the complexity of inorganic mineral–organic matter intergrowth (CIG) acts as a secondary influencing factor.

(3) Of the three coking middling coals, the ground products of CZ displayed the highest organic matter monomer liberation, followed by LW, with SQ showing the lowest. When the particle size decreased from 100 μm to 30 μm, the increase in organic matter liberation was greatest for LW (39.47%), followed by CZ (31.68%), and then SQ (24.23%). The analysis reveals that the complexity of inorganic mineral–organic matter intergrowth (CIG) is the primary factor controlling organic matter liberation.

(4) When the organic matter liberation in LW reached 36.61% and the inorganic mineral liberation reached 77.71%, the flotation efficiency improved significantly. In contrast, as the liberation of organic matter and inorganic minerals increased in CZ and SQ, flotation performance progressively deteriorated.

Author Contributions: Y.H.: Formal Analysis, Methodology, Data Curation, Conceptualization, and Writing—Original Draft. W.L.: Writing—Review and Editing, Project Administration, Methodology, and Conceptualization. Q.Z.: Writing—Review and Editing, Supervision, and Formal Analysis. All authors have read and agreed to the published version of the manuscript.

Funding: This research was funded by the National Natural Science Foundation of China (No. 52104281), the Fundamental Research Funds for the Central Universities (No. 2025ZKPYHH03), and the National Key R&D Program of China (No. 2022YFC2904603).

Data Availability Statement: The original contributions presented in this study are included in the article. Further inquiries can be directed to the corresponding author.

Conflicts of Interest: The authors declare no conflicts of interest.

Abbreviations

The following abbreviations are used in this manuscript:

SEM	Scanning electron microscopy
LW	Liuwan coking middling coal
CZ	Chang Zhi coking middling coal
SQ	Sha Qu coking middling coal
D	Equivalent diameter
AR	Aspect ratio
CIG	Complexity of inorganic–organic intergrowth
TLM	Total degree of inorganic mineral liberation degree
TLO	Total degree of organic matter liberation
CLM	Percentage increase in inorganic mineral liberation content
CLO	Percentage increase in organic matter liberation content

Appendix A

Table A1. Floating selection effectiveness of LW with different average particle sizes under varied collector dosages using the "one coarse, two fine" flotation process.

Average Particle Size d (μm)	Collector Dosage (g/t)	Rough				One Clean				Two Clean				Total Ash (%)	Combustible Recovery (%)
		Tailings		Concentrate		Cleaner Tailings 1		Concentrate		Cleaner Tailings 2		Final Concentrate			
		Yield (%)	Ash (%)	Yield (%)	Ash (%)	Yield (%)	Ash (%)	Yield (%)	Ash (%)	Yield (%)	Ash (%)	Yield (%)	Ash (%)		
170	1800.00	15.99	60.30	84.01	25.64	63.88	42.64	72.68	22.99	17.31	30.63	55.37	20.60	31.18	63.88
	1400.00	14.55	63.55	85.45	26.07	60.74	40.83	69.19	22.60	17.29	30.84	51.90	19.86	31.52	60.74
	1000.00	17.60	60.46	82.39	24.89	53.65	37.08	63.30	21.22	17.89	27.70	45.41	18.66	31.15	53.65
	600.00	13.71	66.64	86.29	25.65	46.28	39.49	68.10	21.96	28.99	26.41	39.10	18.65	31.27	46.28
	200.00	42.03	44.72	57.97	22.56	25.96	27.59	33.56	18.91	12.10	21.23	21.46	17.60	31.88	25.96
	100.00	70.00	35.74	30.00	22.84	9.07	25.88	13.32	19.04	5.94	22.50	7.38	16.25	31.87	9.07
100	1000.00	16.22	63.78	83.78	25.39	66.88	42.87	68.38	21.45	11.79	32.32	56.59	19.18	31.61	66.88
	600.00	37.40	47.33	62.60	22.80	45.41	33.24	47.80	19.57	10.26	26.35	37.54	17.71	31.97	45.41
	200.00	38.49	45.42	61.51	22.55	37.06	30.48	41.39	18.69	10.62	22.71	30.77	17.31	31.35	37.06
	100.00	48.55	43.87	51.45	19.45	29.19	23.52	32.36	17.05	8.77	22.57	23.59	15.00	31.31	29.19
60	1000.00	18.48	58.46	81.52	25.90	62.54	40.90	64.69	22.00	11.70	32.67	52.99	19.64	31.91	62.54
	600.00	31.75	42.71	68.25	26.10	40.40	35.22	46.37	21.80	11.91	28.29	34.46	19.56	31.38	40.40
	200.00	31.03	44.40	68.97	23.47	43.84	33.16	51.19	20.10	13.55	24.75	37.64	18.43	29.96	43.84
	100.00	46.48	41.41	53.52	22.16	29.03	29.03	35.42	18.64	11.64	24.23	23.78	15.91	31.11	29.03
40	1000.00	25.87	45.14	74.13	26.95	53.54	38.84	57.96	23.63	11.50	33.28	46.46	21.24	31.65	53.54
	600.00	31.02	44.38	68.98	25.82	43.39	32.64	51.33	23.48	13.49	28.96	37.83	21.52	31.58	43.39
	200.00	42.47	42.06	57.53	25.00	28.55	30.21	34.63	21.56	10.55	25.88	24.08	19.67	32.25	28.55
	100.00	38.99	40.63	61.01	26.59	30.28	31.69	39.33	23.78	13.04	27.87	26.29	21.75	32.07	30.28
30	2000.00	26.09	42.57	73.91	28.34	42.07	32.24	51.55	26.64	13.70	32.62	37.85	24.48	32.05	42.07
	1600.00	21.74	44.33	78.26	28.17	47.55	33.89	55.68	25.85	12.69	30.58	43.00	24.45	31.68	47.55
	1400.00	30.28	40.50	69.72	27.08	35.25	32.64	45.16	24.06	14.14	29.12	31.02	21.76	31.15	35.25
	1000.00	38.51	38.38	61.49	27.45	27.66	31.59	40.29	25.27	15.80	29.07	24.49	22.81	31.66	27.66
	600.00	31.24	41.82	68.76	27.22	30.56	30.36	47.31	25.80	19.75	27.77	27.57	24.39	31.78	30.56
	200.00	40.89	37.81	59.11	28.29	36.06	34.05	42.58	26.05	10.16	30.81	32.42	24.56	32.18	36.06
	100.00	43.79	37.37	56.21	28.24	22.86	33.77	35.48	25.01	15.48	28.18	20.00	22.56	32.24	22.86

Table A2. Floating selection effectiveness of CZ with different average particle sizes under varied collector dosages using the "one coarse, two fine" flotation process.

Average Particle Size d (μm)	Collector Dosage (g/t)	Rough				One Clean				Two Clean				Total Ash (%)	Combustible Recovery (%)
		Tailings		Concentrate		Cleaner Tailings 1		Concentrate		Cleaner Tailings 2		Final Concentrate			
		Yield (%)	Ash (%)	Yield (%)	Ash (%)	Yield (%)	Ash (%)	Yield (%)	Ash (%)	Yield (%)	Ash (%)	Yield (%)	Ash (%)		
178	1800.00	26.06	65.43	73.94	25.63	19.89	43.13	54.05	19.20	17.71	22.46	36.34	17.61	36.01	46.79
	1400.00	34.05	57.31	65.95	25.24	20.49	37.82	45.46	19.57	9.22	30.12	36.24	16.89	36.16	47.18
	1000.00	40.19	54.80	59.81	23.78	20.84	35.53	38.97	17.49	11.70	24.26	27.27	14.59	36.25	36.54
	200.00	59.10	45.51	40.90	23.61	18.42	30.96	22.49	17.58	7.90	23.26	14.58	14.51	36.55	19.64
	50.00	63.19	46.15	36.81	21.45	18.25	27.75	18.56	15.26	7.36	20.31	11.20	11.94	37.06	15.67
100	1000.00	30.65	62.80	69.36	25.79	15.97	45.34	53.39	19.94	9.67	34.77	43.72	16.66	37.13	57.95
	200.00	52.28	50.27	47.72	24.20	18.70	32.92	29.02	18.57	11.15	25.06	17.86	14.52	37.83	24.56
	100.00	51.33	49.91	48.67	24.70	18.57	33.96	30.10	18.98	9.66	27.82	20.45	14.80	37.64	27.94
	50.00	52.18	47.77	47.82	24.11	19.12	34.89	28.70	16.94	9.30	25.55	19.41	12.81	36.46	26.63
60	1000.00	26.88	62.26	73.12	27.65	11.50	51.42	61.63	23.22	10.88	41.17	50.75	19.37	36.96	64.91
	200.00	42.98	50.00	57.02	25.99	15.66	40.42	41.37	20.54	9.92	32.38	31.45	16.80	36.31	41.08
	100.00	46.46	51.88	53.54	24.71	17.48	33.58	36.06	20.42	9.51	31.21	26.55	16.55	37.33	35.35
	50.00	51.30	49.64	48.70	24.30	14.72	37.45	33.99	18.60	9.83	27.99	24.15	14.78	37.30	32.82
40	1000.00	22.04	58.46	77.96	31.00	18.66	50.58	59.30	24.83	10.39	43.49	48.91	20.87	37.05	61.48
	200.00	39.46	52.94	60.54	28.26	21.19	40.66	39.35	21.58	10.22	31.39	29.13	18.13	37.99	38.46
	100.00	39.18	51.68	60.82	28.06	22.49	36.62	38.34	23.04	13.55	29.10	24.79	19.73	37.31	31.74
	50.00	45.42	49.14	54.58	26.50	20.99	35.66	33.59	20.78	10.44	27.57	23.15	17.72	36.78	30.13
30	1000.00	34.09	49.22	65.91	31.26	18.89	41.70	47.02	27.06	11.43	38.88	35.59	23.27	37.38	43.61
	200.00	43.10	47.15	56.90	29.71	18.87	37.90	38.04	25.65	15.21	30.41	22.82	22.47	37.23	28.19
	100.00	39.22	46.39	60.78	31.34	24.95	38.35	35.83	26.46	12.90	33.59	22.94	22.46	37.25	28.35
	50.00	46.28	45.15	53.72	30.02	24.78	34.97	28.94	25.77	10.80	31.06	18.14	22.62	37.02	22.29

Table A3. Floating selection effectiveness of SQ with different average particle sizes under varied collector dosages using the "one coarse, two fine" flotation process.

Average Particle Size d (μm)	Collector Dosage (g/t)	Rough				One Clean				Two Clean				Total Ash (%)	Combustible Recovery (%)
		Tailings		Concentrate		Cleaner Tailings 1		Concentrate		Cleaner Tailings 2		Final Concentrate			
		Yield (%)	Ash (%)	Yield (%)	Ash (%)	Yield (%)	Ash (%)	Yield (%)	Ash (%)	Yield (%)	Ash (%)	Yield (%)	Ash (%)		
187	1800.00	20.44	70.50	79.56	31.59	14.43	45.56	65.13	28.49	12.26	37.26	52.87	26.46	39.54	64.31
	1400.00	19.05	75.33	80.95	31.20	17.28	42.55	63.67	28.12	17.65	34.46	46.02	25.69	39.61	56.63
	1000.00	26.67	64.18	73.32	31.16	20.75	42.24	52.57	26.78	15.34	33.23	37.23	24.12	39.96	47.05
	600.00	26.89	65.50	73.11	29.88	27.82	35.78	45.28	26.25	13.45	31.07	31.84	24.21	39.46	39.86
	100.00	47.36	52.97	52.64	28.18	20.72	33.58	31.92	24.67	11.54	28.36	20.38	22.58	39.92	26.26
	50.00	43.47	54.66	56.53	29.47	23.66	34.97	32.87	25.50	13.37	29.19	19.49	22.97	40.42	25.20
100	1000.00	20.57	62.98	79.43	34.07	18.07	51.68	61.36	28.89	14.01	38.47	47.35	26.05	40.02	58.38
	200.00	45.71	48.72	54.29	31.01	21.40	37.71	32.90	26.65	11.98	30.68	20.92	24.34	39.10	25.99
	100.00	46.03	50.93	53.97	33.18	23.53	39.53	30.43	28.27	11.66	34.17	18.77	24.60	41.35	24.13
60	1000.00	16.75	77.44	83.26	32.44	15.15	48.67	68.10	28.83	15.08	38.29	53.02	26.14	39.98	65.25
	200.00	49.41	48.19	50.59	31.98	23.51	37.18	27.09	27.47	10.40	31.90	16.68	24.70	39.99	20.93
	100.00	49.15	50.72	50.85	31.16	21.40	37.27	29.45	26.72	9.95	31.74	19.50	24.16	40.77	24.97
40	1000.00	24.82	53.33	75.19	36.38	20.23	44.57	54.95	33.37	17.72	40.32	37.23	30.06	40.59	43.83
	200.00	47.47	49.50	52.53	33.94	25.49	37.93	27.04	30.18	12.33	33.49	14.71	27.41	41.33	18.20
	100.00	45.50	48.48	54.50	34.86	25.94	39.28	28.56	30.85	12.72	35.69	15.85	26.97	41.06	19.64
30	1000.00	34.97	49.72	65.03	36.16	24.87	41.34	40.16	32.95	15.75	36.85	24.41	30.44	40.90	28.73
	200.00	47.68	46.39	52.32	36.50	30.77	39.03	21.54	32.89	10.25	36.08	11.30	29.99	41.22	13.46
	100.00	47.57	44.41	52.43	35.82	26.32	38.93	26.11	32.69	12.25	36.88	13.86	28.98	39.91	16.38

References

1. Yang, Z.; Xia, Y.; Wei, C.; Cao, Y.; Sun, W.; Liu, P.; Cheng, H.; Xing, Y.; Gui, X. New flotation flowsheet for recovering combustible matter from fine waste coking coal. *J. Clean. Prod.* **2019**, *225*, 209–219. [CrossRef]
2. Oki, T.; Yotsumoto, H.; Owada, S. Calculation of degree of mineral matter liberation in coal from sink–float separation data. *Miner. Eng.* **2004**, *17*, 39–51. [CrossRef]
3. Xie, W.; He, Y.; Luo, C.; Zhang, X.; Li, H.; Yu, J.; Wang, H.; Shi, F. Comparison of float-sink and progressive release flotation of ground products of coal middlings. *Physicochem. Probl. Miner. Process.* **2015**, *51*, 675–684.
4. Zou, W.; Cao, Y.; Zhang, Z.; Liu, J. Coal petrology characteristics of middlings from Qianjiaying fat coal mine. *Int. J. Min. Sci. Technol.* **2013**, *23*, 777–782. [CrossRef]
5. Austin, L. Patterns of liberation of ash from coal. *Min. Metall. Explor.* **1994**, *11*, 148–159. [CrossRef]
6. Bu, X.; Chen, Y.; Ma, G.; Sun, Y.; Ni, C.; Xie, G. Differences in dry and wet grinding with a high solid concentration of coking coal using a laboratory conical ball mill: Breakage rate, morphological characterization, and induction time. *Adv. Powder Technol.* **2019**, *30*, 2703–2711. [CrossRef]
7. Huang, Q.; Noble, A.; Talan, D. Exploratory investigation on the use of low-cost alternative media for ultrafine grinding of coal. *Int. J. Coal Prep. Util.* **2022**, *42*, 2127–2144. [CrossRef]
8. Yue, Z.; Li, C.; Han, X.; Ren, R. Evaluation of the Liberation Characteristic of Coarse Middling Coking Coal by Size-Density Fractionation. *Min. Metall. Explor.* **2023**, *40*, 517–528. [CrossRef]
9. Guo, K.; Zhang, D.; Guo, W.; Li, Y.; Xing, Y.; Gui, X. Impact of grinding media shape on the dissociation characteristics and flotation behavior of coking coal middlings. *Powder Technol.* **2025**, *449*, 120423. [CrossRef]
10. Gu, R.; Li, C.; Lu, Q.; Tong, Z.; Sun, X.; Ma, G.; Bu, X.; Sha, J.; Xie, G.; Ulusoy, U. Effect of grinding methods on slime dissociation characteristics and flotation kinetics of coking coal. *Powder Technol.* **2025**, *452*, 120508. [CrossRef]
11. Xie, W.; He, Y.; Zhu, X.; Ge, L.; Huang, Y.; Wang, H. Liberation characteristics of coal middlings comminuted by jaw crusher and ball mill. *Int. J. Min. Sci. Technol.* **2013**, *23*, 669–674. [CrossRef]
12. Gui, X.; Yang, Z.; Xing, Y.; Wang, D.; Ran, J. Liberation properties of middling coking coal under shear force. *Powder Technol.* **2017**, *319*, 483–493. [CrossRef]
13. Hua, Y.; Liu, W.; Zhuo, Q.; Zhang, Y. Identification and quantitative characterization of inorganic mineral embedding features in coking middling coals. *Fuel* **2026**, *404*, 136413. [CrossRef]
14. Sriramoju, S.; Suresh, A.; Dash, P. Generation of low ash fine clean coal powder by autogenous grinding process powder technology. *Powder Technol.* **2019**, *342*, 67–72. [CrossRef]
15. Xie, W.; He, Y.; Wang, Y.; Ge, Z.; Wang, S.; Wang, H. Comparison of flotation behavior of middling coal ground by wet-milling with different media. *Part. Sci. Technol. Int. J.* **2017**, *35*, 616–620. [CrossRef]
16. Cheng, G.; Liu, J.T.; Gui, X.H.; Hu, Z.B.; Wang, Y.T. Effect of different grinding conditions on the dissociation and flotation of difficult-to-float coal. *Energy Sources Part A Recovery Util. Environ. Eff.* **2016**, *38*, 1103–1109.
17. Gautam, S.; Gautam, A.; Patel, M.; Parmar, H.; Patel, K. A statistical analysis and optimization of Indian coal grinding in a laboratory ball mill: Dry & wet method. *Bulg. Chem. Commun.* **2021**, *53*, 51–61.
18. Peng, Y.; Liang, L.; Tan, J.; Sha, J.; Xie, G. Effect of flotation reagent adsorption by different ultra-fine coal particles on coal flotation. *Int. J. Miner. Process.* **2015**, *142*, 17–21. [CrossRef]
19. Gui, X.; Liu, J.; Cao, Y.; Xing, Y.; Deng, Y.; Li, S. Effect of intergrown particle liberation on difficult-to-separate coking coal flotation. *Physicochem. Probl. Miner. Process.* **2016**, *52*, 279–294.
20. Xing, Y.; Xu, X.; Gui, X.; Cao, Y.; Xu, M. Effect of kaolinite and montmorillonite on fine coal flotation. *Fuel* **2017**, *195*, 284–289. [CrossRef]
21. Zhu, Z.; Yin, W.; Li, Z.; Zhang, C.; Wang, D.; Yang, B. Investigation on the liberation and flotation behaviors of coking middlings. *Energy Sources Part A Recovery Util. Environ. Eff.* **2020**, *42*, 536–542.
22. Li, Y.; Xia, W.; Peng, Y.; Li, Y.; Xie, G. Effect of ultrafine kaolinite particles on the flotation behavior of coking coal. *Int. J. Coal Sci. Technol.* **2020**, *7*, 623–632. [CrossRef]
23. Guo, H.; Huang, L.; Liu, X.; Wang, L.; Xia, Y.; Cao, Y.; Gui, X.; Xing, Y. Effect of different mass proportions of fine slime on the flotation performance of coal. *Int. J. Coal Prep. Util.* **2023**, *43*, 1863–1884. [CrossRef]
24. Chary, G.; Dastidar, M. Optimization of experimental conditions for recovery of coking coal fines by oil agglomeration technique. *Fuel* **2010**, *89*, 2317–2322. [CrossRef]
25. Xia, W.; Li, Y.; Wu, F.; Niu, C. Enhanced flotation selectivity of fine coal from kaolinite by anionic polyacrylamide pre-conditioning. *J. Mol. Liq.* **2021**, *334*, 116083. [CrossRef]
26. Hazare, G.; Pradhan, S.S.; Dash, N.; Dwari, R.K. Studies on low-grade coking coal characterisation, flotation response and process optimisation. *Int. J. Coal Prep. Util.* **2023**, *43*, 2165–2187. [CrossRef]
27. Wills, B.A.; Finch, J. *Wills' Mineral Processing Technology: An Introduction to the Practical Aspects of Ore Treatment and Mineral Recovery*; Butterworth-Heinemann: Oxford, UK, 2015.

28. Qu, K.; Yuan, Z.; Wang, Y.; Song, Z.; Gong, X.; Zhao, Y.; Mu, Q.; Zhan, Q.; Xu, W.; Wang, L. Structures, properties, and applications of zwitterionic polymers. *ChemPhysMater* **2022**, *1*, 294–309. [CrossRef]
29. Sahoo, B.; Gouda, M.; Nayak, C. Demineralization of fine and ultrafine coal particles of Talcher area by oil agglomeration technique. *Int. J. Coal Prep. Util.* **2024**, *44*, 2225–2239. [CrossRef]
30. Ma, L.; Wu, L.; Ye, G.; Sun, X. The role of surface cleaning in high intensity conditioning. *Powder Technol.* **2017**, *319*, 26–33. [CrossRef]
31. Mei, Y.; Lin, Q.; Cao, D.; Li, J.; Liu, K. Enhancement of ultrafine coal slime flotation using high-shear pretreatment and polyvinylpyrrolidone. *Int. J. Coal Prep. Util.* **2023**, *43*, 2136–2151. [CrossRef]
32. Cheng, G.; Li, Y.; Cao, Y.; Zhang, Z. A novel method for the desulfurization of medium–high sulfur coking coal. *Fuel* **2023**, *335*, 126988. [CrossRef]
33. Zhang, H.; Bai, J.; Kong, L.; Li, X.; Bai, Z.; Li, W. Behavior of minerals in typical Shanxi coking coal during pyrolysis. *Energy Fuels* **2015**, *29*, 6912–6919. [CrossRef]
34. Little, L.; Mainza, A.N.; Becker, M.; Wiese, J.G. Using mineralogical and particle shape analysis to investigate enhanced mineral liberation through phase boundary fracture. *Powder Technol.* **2016**, *301*, 794–804. [CrossRef]

Disclaimer/Publisher's Note: The statements, opinions and data contained in all publications are solely those of the individual author(s) and contributor(s) and not of MDPI and/or the editor(s). MDPI and/or the editor(s) disclaim responsibility for any injury to people or property resulting from any ideas, methods, instructions or products referred to in the content.